Krill body size drives particulate organic carbon export in West Antarctica

https://doi.org/10.1038/s41586-023-06041-4

Rebecca Trinh^{1,2 ⊠}, Hugh W. Ducklow^{1,2}, Deborah K. Steinberg³ & William R. Fraser⁴

Received: 18 January 2022

Accepted: 31 March 2023

Published online: 14 June 2023



Check for updates

The export of carbon from the ocean surface and storage in the ocean interior is important in the modulation of global climate¹⁻⁴. The West Antarctic Peninsula experiences some of the largest summer particulate organic carbon (POC) export rates, and one of the fastest warming rates, in the world^{5,6}. To understand how warming may alter carbon storage, it is necessary to first determine the patterns and ecological drivers of POC export^{7,8}. Here we show that Antarctic krill (Euphausia superba) body size and life-history cycle, as opposed to their overall biomass or regional environmental factors, exert the dominant control on the POC flux. We measured POC fluxes over 21 years, the longest record in the Southern Ocean, and found a significant 5-year periodicity in the annual POC flux, which oscillated in synchrony with krill body size, peaking when the krill population was composed predominately of large individuals. Krill body size alters the POC flux through the production and export of size-varying faecal pellets⁹, which dominate the total flux. Decreases in winter sea ice¹⁰, an essential habitat for krill, are causing shifts in the krill population¹¹, which may alter these export patterns of faecal pellets, leading to changes in ocean carbon storage.

Collectively referred to as the biological pump¹, the process of biological production, aggregation and export of particulate organic carbon (POC) from the euphotic zone to the ocean interior is important in global biogeochemical cycles^{12,13}, helping to redistribute carbon and nutrients within the ocean, and playing an integral role in modulating atmospheric carbon dioxide (CO₂) concentrations²⁻⁴. Though it only comprises 20% of the global ocean surface area, the Southern Ocean is a region of major global biogeochemical relevance, in which it accounts for an estimated 30% of the global annual oceanic carbon export, about 1.5-3 PgC yr⁻¹ (ref. 14). Despite a long history of investigation of Southern Ocean ecology, most observations of POC export are limited to ice-free seasons and to individual years, with few winter or multi-year records $^{15-17}$. This relative dearth of in situ measurements limits our understanding of seasonal and interannual variability and long-term trends in POC export. Moored sediment traps provide one of the few sources of year-round observations of biogeochemical dynamics in the ocean interior, especially in hard-to-sample areas such as the polar marginalice zones (MIZs). Long-term sediment-trap time series of the sinking particle flux are thus an irreplaceable component of the assessment of the drivers of the biological pump, and potential changes to carbon export and sequestration 18-20.

Here we present an analysis of sediment-trap data from the MIZ of the West Antarctic Peninsula (WAP; Extended Data Fig. 1) in the Southern Ocean. The MIZ is characterized by intensified biological activity, high sedimentation and deep seasonal drawdown of CO₂ (refs. 5,6,21,22). The WAP has experienced a 6 °C increase in mean atmospheric temperature since 1950, during the critical winter months, leading to the deterioration of sea-ice cover^{10,23,24}, which provides the foundation for all aspects of the WAP biological pump. Understanding how climate change will alter the Southern Ocean sea-ice concentration, POC export, and atmospheric CO₂ uptake is thus a critical scientific priority^{7,8}.

Winter sea ice on the WAP provides a critical habitat for Antarctic krill (Euphausia superba). E. superba comprises the highest concentration of animal biomass of a singular species in the world²⁵ and is a key species in the Antarctic food web²⁶. Furthermore. E. superba is one of the largest and longest-lived epipelagic zooplankton, reaching an average of about 60 mm in length by the end of their five-to-six-vear life cycle. As such a unique organism, krill play an outsized role in Antarctic biogeochemical cycles through their grazing and egestion of large, carbon-rich, fast-sinking faecal pellets (FPs)^{9,27}. Krill FPs can sink hundreds of metres per day, making them readily exported out of the surface layer and an important courier of carbon from the euphotic zone to the ocean interior $^{28-30}$.

Our analysis compares patterns in the multi-decadal sediment-trap time series (1992-2013; Fig. 1) of POC flux on the continental shelf of the WAP to krill population dynamics. The sediment trap is moored at about 350 m water depth and continuously intercepts sinking particles at 170 m depth. This record is the longest time series of POC export in the Southern Ocean, with year-round collection of sinking particles, including during austral winter and under sea-ice cover, and is thus sensitive to ecologically important seasonal-to-decadal processes. We quantify interannual patterns in the POC flux, and find that krill life history and body size, as opposed to their numerical density and biomass, are drivers of carbon export on the WAP through their production and subsequent export of size-varying, carbon-rich FPs.

Deparment of Earth and Environmental Sciences, Columbia University, New York, NY, USA. ²Lamont-Doherty Earth Observatory, Columbia University, Palisades, NY, USA. ³Virginia Institute of Marine Science, William & Mary, Gloucester Point, VA, USA. ⁴Polar Oceans Research Group, Sheridan, MT, USA. ™e-mail: rtrinh@ldeo.columbia.edu

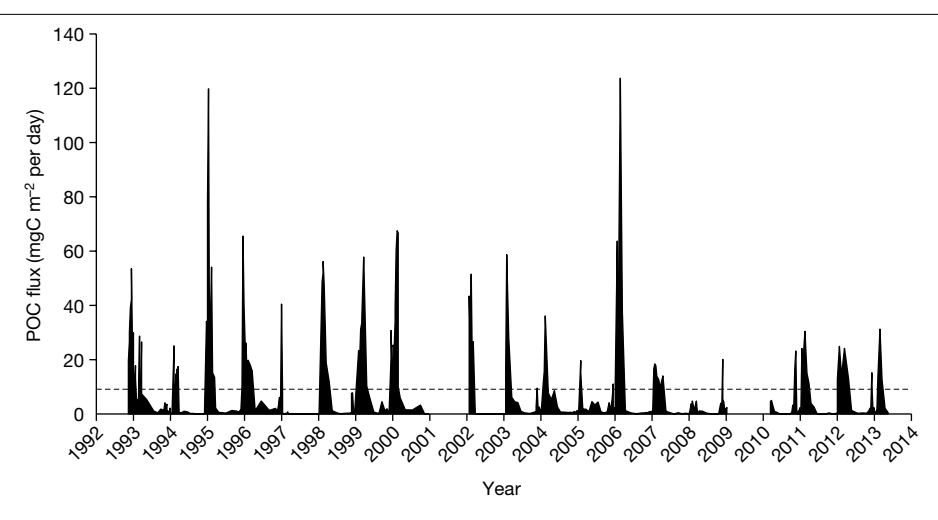


Fig. 1 | WAPPOC flux time series from 1992 to 2013. The black dashed line shows the mean daily POC flux rate. The x-axis tick marks denote 1 January of each year.

Interannual variability in POC flux

The mean annual (July–June; Methods) POC flux over the 21-year time series was 2.3 ± 1.3 gC m⁻², but varied over an order of magnitude, between 0.3 gC m⁻² and 5.3 gC m⁻², where each year was characterized by a pronounced summer peak in the flux of varying amplitude (Fig. 1). The annual POC flux accounted for an average of $13.6 \pm 10.8\%$ of the annual total mass flux. Our median annual POC flux (2.13 gC m⁻²) is twice the estimated global median POC flux of about 1 gC m⁻² (ref. 31). An average of $80 \pm 23\%$ of the annual POC flux occurs within the peak initiation-to-termination period, indicating that the vast majority of the annual flux accumulation occurs during less than one-sixth of the year, specifically, during the austral spring-summer period.

The annual POC flux oscillated between strongly positive and strongly negative anomalies (Fig. 2a). Anomalously high export years occurred five to six years apart (1994, 1999 and 2005; Fig. 2a). There is no significant linear decrease in POC export over the two decades analysed ($R^2 = 0.023$, P = 0.59). Increase in annual peak flux duration time did not correlate with higher annual POC flux (Extended Data Fig. 2: $R^2 = 0.025$, P = 0.54). Spectral analysis of the annual POC flux confirmed a significant five-year periodicity in the POC flux time series (Fig. 2b; P < 0.001).

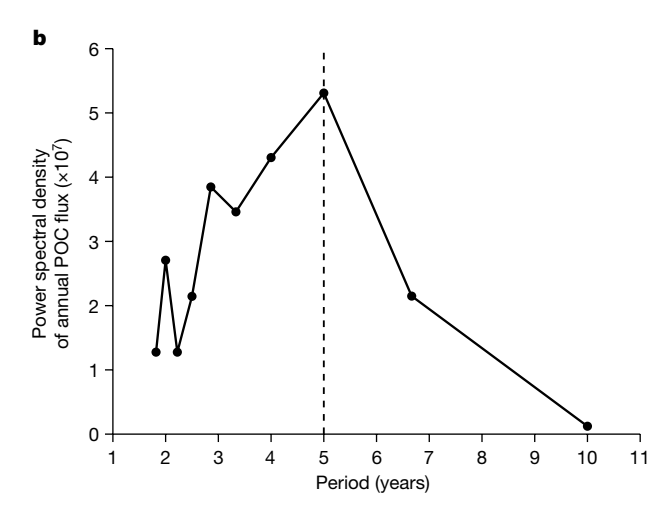
2.0 1.5 Annual mean POC flux anomaly 1.0 0.5 0 -0.5 -1.01992 1994 1996 1998 2000 2002 2004 2006 2008 2010 2012

Fig. 2 | Annual POC flux oscillates on a five-year periodicity. a, Mean annual standardized POC flux anomaly. The x-axis tick marks denote the start of each July-June flux year. b, Spectral analysis of annual POC flux data. The analysis

Krill body size and annual POC flux

The semi-decadal oscillation of the POC flux on the WAP was not correlated with interannual variability in sea-ice cover or sub-decadal climate oscillation such as El Niño-Southern Oscillation (ENSO) and the Southern Annular Mode (SAM; Extended Data Table 1). Phytodetritus constituted only a small percentage of the summer POC flux, but this increased in proportion during the winter months³⁰ when krill are less likely to be found over the WAP continental shelf. However, there was not a significant correlation between summer phytoplankton biomass (chlorophyll a) and POC export over the two decades (Extended Data Table 1). Salps are another common Antarctic zooplankton that oscillate in total abundance in connection with varying oceanographic conditions. Salps can produce large, carbon-rich FPs³²; however, on the WAP, these FPs may be prone to breakage and disaggregation while sinking through the water column^{33,34} and there was no correlation between POC export on the WAP and salp abundance (Extended Data Table 1).

Analysis of FPs from a five-year subset of this time series (January 2004 to January 2009) indicates that the cylindrical FPs of E. superba contribute the most in terms of both the absolute number and the total POC contribution to the annual POC export on the WAP³⁰. These cylindrical FPs constituted on average 72% overall, and 82% in summer



indicates a five-year periodicity (P < 0.001, Bartlett's Kolmogorov-Smirnov statistic⁵¹). The dashed line at five years is for reference.

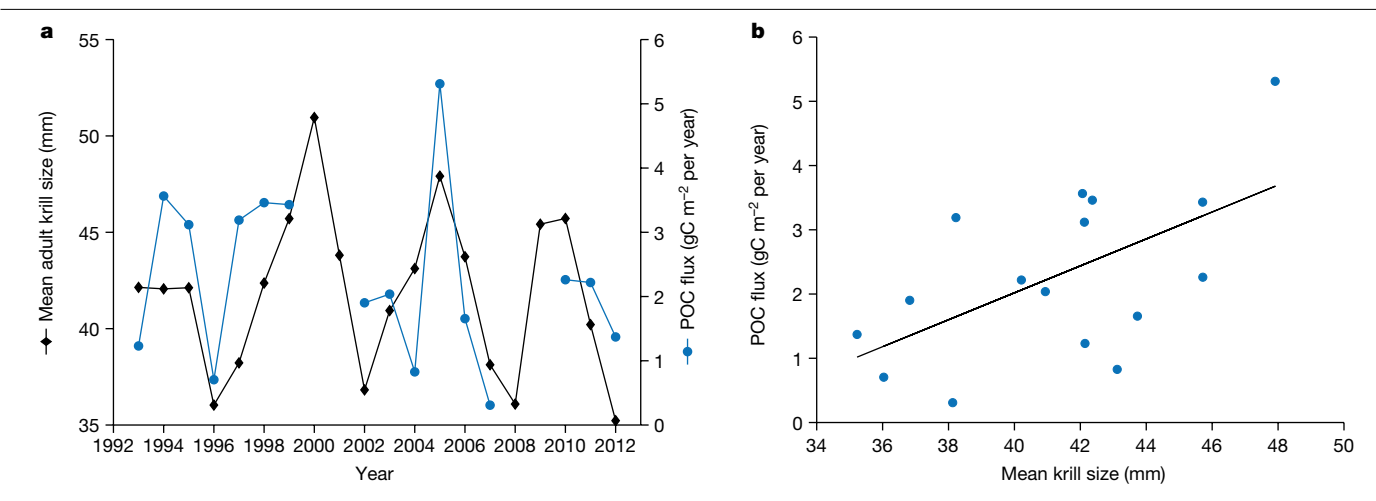


Fig. 3 | **Summer Antarctic krill body size drives annual POC flux. a**, Annual POC flux (blue circles) and annual mean adult *E. superba* body size (black diamonds) from 1993 to 2012. The *x*-axis tick marks denote the start of each

July–June year. **b**, Annual POC flux as a function of annual mean adult krill body size $(R^2 = 0.34, P = 0.018)$.

months, of the total POC flux³⁰. We found that the total POC flux was driven by the overall amount of cylindrical krill FPs, regardless of whether it was a high or low total POC flux year. Regardless of whether a flux year was anomalously high or anomalously low, the proportion of cylindrical krill FPs remained high, especially during austral summer months.

Although krill and their FPs are a major contributor to the POC flux on the WAP, the summer total krill abundance was not significantly correlated with the integrated annual POC flux (Extended Data Fig. 3a,b), and although they appear antiphased, the negative relationship between total E. superba abundance and POC flux was also not significant (Extended Data Fig. 3b; $R^2 = 0.15$, P = 0.13). Furthermore, there was also no correlation between adult (>30 mm) krill abundance and the annual POC flux (Extended Data Fig. 4a,b; $R^2 = 0.063$, P = 0.35).

Rather, adult krill body size (length) was the most significant factor related to the annual POC flux. The annual POC flux oscillates in synchrony with the mean summer adult E. Superba body size, reaching a maximum every five to six years (Fig. 3a), with the POC flux significantly positively correlated with adult body size (Fig. 3b; $R^2 = 0.34$, P = 0.018). Anomalously high annual POC flux occurred when the krill population was dominated by larger (older) adult krill, where $63.5\% \pm 12\%$ of the krill population was composed of large adults ≥ 41 mm in length, matching the length–frequency distribution of a population composed of age classes four years and older 35,36 . Years of anomalously low POC flux coincided with years following high juvenile krill recruitment, matching the length–frequency distribution of a population composed of age classes two years and younger 35,36 .

Analysis of krill body size from Adélie penguin diet contents over the same 21-year period also indicates that krill body size oscillates over a 5-year cycle, in synchrony with both net-tow krill body size and the POC flux on the WAP (Extended Data Fig. 5). Krill body size observed in penguin diets was also significantly positively correlated with the POC flux (Extended Data Fig. 6; R^2 = 0.36, P = 0.01). The use of independent krill sampling methods through abiotic and biotic means, net-tows and predator diet samples, respectively, further supports the robustness of the krill body size pattern on the WAP and its influence on POC export.

Our study demonstrates that the oscillatory pattern of the interannual POC flux magnitude on the WAP follows a five-year cycle and is mechanistically linked to the summer body size of the adult *E. superba*, as opposed to total krill abundance or to other biological and environmental factors, including other zooplankton abundance, phytoplankton biomass, and sea-ice cover. The annual total *E. superba* abundance

is significantly negatively correlated with the annual mean krill body size when all size classes of krill are taken into account in both net tows (Extended Data Fig. 7a; $R^2 = -0.50$, P < 0.001) and Adélie penguin diets (Extended Data Fig. 7b; $R^2 = -0.45$, P = 0.001). This indicates that during years of high krill abundance, the population is made up of mostly young, small krill and helps to explain why there is no significant relationship between total *E. superba* abundance and annual POC flux (Extended Data Figs. 3 and 4).

We propose that the semi-decadal cycle in POC flux is intimately linked to the krill life cycle. On the WAP, the Antarctic krill population is dominated by a strong age-class structure, with individuals within a cohort recruiting, ageing and growing in body size together over multiple years 36-39. The five-year cycle in POC flux in our analysis matches the five-year cycle in krill size class 38 and is antiphased with the five-year cycle of krill abundance, with peaks in abundance occurring after larval recruitment 40. The winter MIZ is an essential habitat for successful recruitment 41, helping to set up the next five-year cycle of the next krill cohort 38.

The continued annual growth, combined with the five-to-six-year longevity of E. superba, means that individual krill within the large cohort grow in body length in near synchrony over the five-year cycle. Because krill possess simple, tube-like, linear guts, they produce long cylindrical pellets that increase in size according to their body length9. Both the length and the width of krill FPs positively correlate with FP POC content³³ and overall density, with FP density additionally influenced by the krill's food source²⁹. The larger, longer FPs produced by older adults are more likely to sink out of the upper mixed layer faster than smaller FPs produced by smaller, younger krill, and to be found in deeper sediment traps^{9,30}. One consequence of the life history of *E. superba* is that the annual POC flux is at a minimum when krill abundance and biomass are peaking, and when the cohort is composed of many young, small juveniles after successful recruitment. Recruitment of the next cohort is affected by complex environmental factors such as ENSO, which oscillates on a semi-decadal timescale, sea-ice cover⁴¹, and biological factors such as quantity and quality of food and resource competition between krill^{39,40}. As the krill cohort ages and grows, the POC flux increases commensurately over the next four to five years.

In the summer, small juvenile krill are found mostly over the inner shelf, whereas the larger, sexually mature adults make a longer ontogenetic migration, congregating over the outer shelf and continental shelf break^{35,42-44}. The seasonal age-specific, and therefore size-specific, habitat preferences of *E. superba* are especially amplified during the summer. The effect of these differential distribution patterns is that

the krill in younger stages are separated from adults. Adult krill play a larger role in summer POC flux over the outer shelf, where the sediment trap is located (Extended Data Fig. 1) through their egestion of large, carbon-rich FPs³⁰, leading to the intense and episodic peak in the POC flux during the summer.

E. superba form large swarms in the upper water column, with swarms containing up to two million tonnes of krill⁴⁵. The swarming and schooling behaviour of E. superba further facilitates the export of FP out of the upper water column by increasing and synchronizing the supply of POC relative to the carbon demand of heterotrophic organisms that degrade and consume organic matter such as FPs as they sink. This process is probably amplified when the krill are larger and their FPs are larger with higher sinking rates 28-30. These intense and episodic FP production events are probably particularly efficient in transferring POC to the ocean's interior. As FPs sink through the water column, there may be physical breakage and fragmentation of pellets, thereby altering their sinking rate. However, even with fragmentation, the potential for longer FPs is greater in years of larger krill than in years dominated by small krill.

In our study, krill size was positively correlated with POC export, as opposed to increased abundance of krill and biomass as suggested by previous work^{46,47}. A negative relationship between *E. superba* abundance and annual mean krill body size (Extended Data Fig. 7a,b) has been shown elsewhere 40. E. superba play a critically important role in POC export and biogeochemical cycles in the Southern Ocean^{18,27,47}; however, using krill abundance densities to estimate krill FP POC flux probably overestimates the contribution of krill FP POC export during years when the krill abundance is high but the population is dominated by small juveniles. Furthermore, using abundance and size data, we find that overall krill biomass in the water column does not correlate with POC export over the two-decade study period.

The mechanistic driver of the POC flux found in our region of the WAP may also be applicable to other MIZs that are dominated by krill. E. superba in the far northern Antarctic Peninsula also exhibit a four-to-six-year cycle in post-larval krill abundance and strong cohort dynamics, similar to that of our study region on the WAP^{36,48,49}. The POC flux in this more northerly region may be similarly characterized by large pulses every four to six years following the cycle of body size of the local krill population, and warrants further research. A poleward shift in the krill population and a lack of successful recruitment of juveniles to replenish the ageing local population have been observed in the Atlantic sector of the Southern Ocean, which includes the WAP¹¹. The spatial contraction of these krill populations is hypothesized to result from increased warming¹¹ and may disrupt the current five-year cycle in krill body size, and thus, may alter the long-standing regional pattern in POC flux. Continued warming could alter the phenology and composition of exported POC, shifting peak pulses to later in the season and increasing the relative proportion of other zooplankton FPs to export, such as salp FPs⁴⁰. Warming is also hypothesized to enhance microbial remineralization of organic matter⁵⁰ in the water column and benthos, thereby decreasing and altering the POC flux, deep carbon storage, and benthic food availability.

Conclusion

The semi-decadal nature of the POC flux that characterizes the WAP continental shelf would be impossible to capture without continuous, long-term export observations. As the longest-running time series of POC flux and Antarctic krill in the Southern Ocean, our observations highlight the importance of understanding the complex life-history strategies of the organisms that power the biological pump and the interplay between them and their sea-ice environment. Krill FPs are rich in organic carbon, less prone to fragmentation and exhibit high sinking rates. Coupled with their distinct ecology, including growth, longevity, swarming behaviour and seasonal migrations, E. superba and

its FPs are a uniquely important component of POC production and export and form the central component of the WAP biological pump. The resident krill population, with its dependence on seaice, make the MIZ of the WAP a region of intense export in the Southern Ocean and an important region for carbon storage.

Online content

Any methods, additional references, Nature Portfolio reporting summaries, source data, extended data, supplementary information, acknowledgements, peer review information; details of author contributions and competing interests; and statements of data and code availability are available at https://doi.org/10.1038/s41586-023-06041-4.

- Volk, T. & Hoffert, M. I. in The Carbon Cycle and Atmospheric CO.; Natural Variations Archean to Present (eds Sundquist, E. & Broecker, W. S.) 99-110 (American Geophysical Union, 1985).
- Sarmiento, J. L., Hughes, T. M., Stouffer, R. J. & Manabe, S. Simulated response of the ocean carbon cycle to anthropogenic climate warming. Nature 393, 245-249 (1998).
- Marinov, I. et al. Impact of oceanic circulation on biological carbon storage in the ocean and atmospheric pCO2. Glob. Biogeochem. Cycles 22, GB3007 (2008).
- Studer, A. S. et al. Increased nutrient supply to the Southern Ocean during the Holocene and its implications for the pre-industrial atmospheric CO2 rise. Nat. Geosci. 11, 756-760
- Honjo, S. in Polar Oceanography (ed Smith, W. O. Jr) 322-353 (Academic, 1990).
- Meredith, M. P., Stefels, J. & van Leeuwe, M. Marine studies at the western Antarctic Peninsula: priorities, progress and prognosis. Deep Sea Res. Part II 139, 1-8 (2017).
- Bopp, L. et al. Potential impact of climate change on marine export production. Glob. Biogeochem. Cycles 15, 81-99 (2001).
- Passow, U. & Carlson, C. A. The biological pump in a high CO2 world. Mar. Ecol. Prog. Ser. 470, 249-271 (2012).
- Cadée, G. C., González, H. & Schnack-Schiel, S. B. Krill diet affects faecal string settling. Polar Biol. 12, 75-80 (1992).
- Stammerjohn, S. & Maksym, T. in Sea Ice 3rd edn (ed. Thomas, D. N.) Ch. 10 (John Wiley & Sons. 2017).
- Atkinson, A. et al. Krill (Euphausia superba) distribution contracts southward during rapid regional warming, Nat. Clim. Change 9, 142-147 (2019).
- Knox, F. & McElroy, M. B. Changes in atmospheric CO₂: influence of the marine biota at high latitude. J. Geophys. Res. Atmos. 89, 4629-4637 (1984).
- 13. Siegel, D. A., DeVries, T., Cetinić, I. & Bisson, K. M. Quantifying the ocean's biological pump and its carbon cycle impacts on global scales. Annu. Rev. Mar. Sci. 15, 329-356 (2022).
- Long, M. C. et al. Strong Southern Ocean carbon uptake evident in airborne observations. Science 374, 1275-1280 (2021).
- Arteaga, L., Haëntjens, N., Boss, E., Johnson, K. S. & Sarmiento, J. L. Assessment of export efficiency equations in the Southern Ocean applied to satellite-based net primary production. J. Geophys. Res. Oceans 123, 2945-2964 (2018).
- Nöthig, E. M. & von Bodungen, B. Occurrence and vertical flux of faecal pellets of probably protozoan origin in the southeastern Weddell Sea (Antarctica). Mar. Ecol. Prog. Ser. 56
- Palangues, A., Isla, E., Puig, P., Sanchez-Cabeza, J. A. & Masgué, P. Annual evolution of downward particle fluxes in the Western Bransfield Strait (Antarctica) during the FRUELA project. Deep Sea Res. Part II 49, 903-920 (2002).
- Manno, C. et al. Continuous moulting by Antarctic krill drives major pulses of carbon export in the north Scotia Sea, Southern Ocean. Nat. Commun. 11, 6051 (2020)
- Karl, D. M. & Lukas, R. The Hawaii Ocean Time-series (HOT) program: background, rationale and field implementation, Deep Sea Res. Part II 43, 129-156 (1996).
- Conte, M. H., Ralph, N. & Ross, E. H. Seasonal and interannual variability in deep ocean particle fluxes at the Oceanic Flux Program (OFP)/Bermuda Atlantic Time Series (BATS) site in the western Sargasso Sea pear Bermuda, Deep Sea Res, Part II 48, 1471-1505 (2001).
- 21. Wynn-Edwards, C. A. et al. Particle fluxes at the Australian Southern Ocean Time Series (SOTS) achieve organic carbon sequestration at rates close to the global median, are dominated by biogenic carbonates, and show no temporal trends over 20-years. Front. Earth Sci. 8, 329 (2020).
- 22. Schofield, O. et al. Decadal variability in coastal phytoplankton community composition in a changing West Antarctic Peninsula. Deep Sea Res. Part I 124, 42-54 (2017).
- Vaughan, D. G. et al. Recent rapid regional climate warming on the Antarctic Peninsula. Climatic Change 60, 243-274 (2003).
- Stammerjohn, S. E. & Scambos, T. A. Warming reaches the South Pole. Nat. Clim. Chang. 10, 710-711 (2020).
- Atkinson, A., Siegel, V., Pakhomov, E. A., Jessopp, M. J. & Loeb, V. A re-appraisal of the total biomass and annual production of Antarctic krill. Deep Sea Res. Part I 56, 727-740
- Loeb, V. et al. Effects of sea-ice extent and krill or salp dominance on the Antarctic food web. Nature 387, 897-900 (1997).
- Cavan, E. L. et al. The importance of Antarctic krill in biogeochemical cycles. Nat. Commun. 10. 4742 (2019).
- McDonnell, A. M. & Buesseler, K. O. Variability in the average sinking velocity of marine particles. Limnol. Oceanogr. 55, 2085-2096 (2010).
- Atkinson, A., Schmidt, K., Fielding, S., Kawaguchi, S. & Geissler, P. A. Variable food absorption by Antarctic krill: relationships between diet, egestion rate and the composition and sinking rates of their fecal pellets, Deep Sea Res, Part II 59, 147-158 (2012).

- Gleiber, M. R., Steinberg, D. K. & Ducklow, H. W. Time series of vertical flux of zooplankton fecal pellets on the continental shelf of the western Antarctic Peninsula. *Mar. Ecol. Prog* Ser. 471, 23–36 (2012).
- Lampitt, R. S. & Antia, A. N. Particle flux in deep seas: regional characteristics and temporal variability. Deep Sea Res. Part I 44, 1377–1403 (1997).
- 32. Décima, M. et al. Salp blooms drive strong increases in passive carbon export in the Southern Ocean. *Nat. Commun.* **14**, 425 (2023).
- Pauli, N. C. et al. Krill and salp faecal pellets contribute equally to the carbon flux at the Antarctic Peninsula. Nat. Commun. 12, 7168 (2021).
- Iversen, M. H. et al. Sinkers or floaters? Contribution from salp pellets to the export flux during a large bloom event in the Southern Ocean. Deep Sea Res. Part II 138, 116–125 (2017)
- Siegel, V., Reiss, C. S., Dietrich, K. S., Haraldsson, M. & Rohardt, G. Distribution and abundance of Antarctic krill (Euphausia superba) along the Antarctic Peninsula. Deep Sea Res. Part 177. 63–74 (2013).
- Reiss, C. S. in Biology and Ecology of Antarctic Krill Advances in Polar Ecology (ed. Siegel, V.) 101–144 (Springer, 2016).
- Siegel, V. Age and growth of Antarctic Euphausiacea (Crustacea) under natural conditions. Mar. Biol. 96, 483–495 (1987).
- Fraser, W. R. & Hofmann, E. E. A predator's perspective on causal links between climate change, physical forcing and ecosystem response. Mar. Ecol. Prog Ser. 265, 1–15 (2003).
- Saba, G. K. et al. Winter and spring controls on the summer food web of the coastal West Antarctic Peninsula. Nat. Commun. 5, 4318 (2014).
- Steinberg, D. K. et al. Long-term (1993–2013) changes in macrozooplankton off the Western Antarctic Peninsula. Deep Sea Res. Part I 101, 54–70 (2015).
- Meyer, B. et al. The winter pack-ice zone provides a sheltered but food-poor habitat for larval Antarctic krill. Nat. Ecol. Evol. 1, 1853–1861 (2017).
- Siegel, V. in Antarctic Ocean and Resources Variability (ed. Sahrhage, D.) 219–230 (Springer, 1988).

- 43. Nicol, S. Krill, currents, and sea ice: *Euphausia superba* and its changing environment. *Bioscience.* **56**, 111–120 (2006).
- Kawaguchi, S. in Biology and Ecology of Antarctic Krill (ed. Siegel, V.) 225–246 (Springer, 2016).
- Tarling, G. A. & Fielding, S. in Biology and Ecology of Antarctic Krill (ed. Siegel, V.) 279–319 (Springer, 2016).
- Belcher, A. et al. Krill faecal pellets drive hidden pulses of particulate organic carbon in the marginal ice zone. Nat. Commun. 10, 889 (2019).
- Belcher, A. et al. The potential role of Antarctic krill faecal pellets in efficient carbon export at the marginal ice zone of the South Orkney Islands in spring. *Polar Biol.* 40, 2001–2013 (2017).
- Fielding, S. et al. Interannual variability in Antarctic krill (Euphausia superba) density at South Georgia, Southern Ocean: 1997–2013. ICES J. Mar. Sci. 71, 2578–2588 (2014).
- Conroy, J. A., Reiss, C. S., Gleiber, M. R. & Steinberg, D. K. Linking Antarctic krill larval supply and recruitment along the Antarctic Peninsula. *Integr. Comp. Biol.* 60, 1386–1400 (2020).
- Cavan, E. L. & Boyd, P. W. Effect of anthropogenic warming on microbial respiration and particulate organic carbon export rates in the sub-Antarctic Southern Ocean. Aquat. Microb. Ecol. 82. 111–127 (2018).
- 51. Fuller, W. A. Introduction to Statistical Time Series 698 (Wiley, 1996).

Publisher's note Springer Nature remains neutral with regard to jurisdictional claims in published maps and institutional affiliations.

Springer Nature or its licensor (e.g. a society or other partner) holds exclusive rights to this article under a publishing agreement with the author(s) or other rightsholder(s); author self-archiving of the accepted manuscript version of this article is solely governed by the terms of such publishing agreement and applicable law.

© The Author(s), under exclusive licence to Springer Nature Limited 2023

Methods

Study region

The Palmer Long-Term Ecological Research (PAL-LTER) project has been studying the marine ecosystem of the WAP since 1992, with long-term observations conducted during the austral summer annually each January–February within the PAL-LTER offshore sampling grid aboard the MV *Polar Duke* (1993–1997) and ARSV *Laurence M. Gould* (1998–2020). The PAL-LTER sampling grid covers a 170,000 km² area of the Bellingshausen Sea (Extended Data Fig. 1), extending approximately 700 km from Palmer Station, Anvers Island (64.77° S, 64.05° W) to Charcot Island (69.45° S, 75.15° W). Grid lines are numbered from –100 to 600 and spaced 100 km apart, and stations within each line are spaced 20 km apart, beginning from the coast to approximately 200 km offshore at the slope/shelf break significant contents.

Sediment trap

As part of the PAL-LTER effort to understand the marine ecology and biogeochemistry of the WAP, a sediment trap (PARFLUX Mark 78H 21-sample traps; McLane Research Labs) has been deployed since November 1992 to collect sinking particles from the biologically productive continental shelf euphotic zone⁵³. The sediment trap is moored at 64.5° S, 66.0° W at about 350 m water depth. It is located about 130 km offshore, on the outer continental shelf, and between the 500 and 600 PAL-LTER grid lines (Extended Data Fig. 1). The trap consists of a large conical funnel, 0.5 m² in opening area with a plastic baffle mounted in the opening to prevent large-sized organisms from swimming into the trap. The trap continuously intercepts sinking particles at 170 m depth. Below the funnel are 21 collection cups filled with a high-density salt solution, 7.5 g l⁻¹NaCl and 2% borate-buffered formalin in filtered seawater (about 34 ppt), with a final concentration of 41 ppt, to retain and preserve sinking material. The trap autonomously collects sinking particles throughout the year into each sampling cup in intervals varying from 4 days to 61 days, with shorter intervals during the expected peak flux in austral summer, and longer intervals during the low biological productivity period in the winter. The deployment location was seasonally covered with sea ice 105 ± 37 days (mean \pm s.d.) per year during the 21-year study period. The trap was recovered and redeployed each January-February during the annual cruise.

Trap sample processing and data analysis

Upon recovery each year, the trap samples were sealed and held at 5 °C until return to the USA for processing. Samples from heavy sediment flux periods were split up to 1/512 with a plankton splitter or wet sample divider (McLane) for subsequent analysis. Zooplankton 'swimmers' were removed from each trap sample before sample analyses. Total mass dry weight, POC and particulate nitrogen were measured for each sample. Detailed methods for zooplankton removal are described in ref. 53 and sediment-trap chemical analyses are described in the Joint Global Ocean Flux Study protocols⁵⁴. Briefly, after removal of zooplankton swimmers and splitting, samples were dried, homogenized and fumed with dilute hydrochloric acid to remove inorganic carbon. POC was measured on CHN analysers. Owing to the multi-decadal nature of PAL-LTER, POC was measured at several institutions on several different CHN analysers: PerkinElmer 2400 (1992-May 1994), Europa Scientific SL (June 1994-1997), Exeter Analytical Elemental Analyzer (1997-2003), Carlo Erba EA 1108 (2003-2007), PerkinElmer 2400 and Thermo Scientific Flash 2000 (2007–2013). Samples were all run against the same standard, acetanilide (C₈H₉NO)^{53,55}. Up to three replicate analyses of chemical properties were performed on each trap sample and the analytical replicates were averaged for each sample. When multiple traps were simultaneously deployed adjacent to each other during the same time frame, samples were averaged for corresponding intervals⁵⁴. These data can be found at https://doi.org/10.6073/pasta/ cb0ee837fd2615ae133dcfdc0b806571.

We report daily POC flux from each year's 21 collection cups from 1992 to 2013 (Fig. 1). To understand the interannual variability in the POC flux and its ecological drivers, the sediment-trap POC flux data were integrated in July-June year format, starting on 1 July of calendar year one, and spanning to 30 June the following year, to avoid systematically splitting up the spring and summer peak flux period (November-March) in which the majority of the POC flux occurs². For example, the July-June year 1996 spans from 1 July 1996 to 30 June 1997 and encompasses the summer peak POC flux period of the austral summer continuously. All annual POC flux data are analysed and presented graphically in this July-June format from Fig. 2 onwards. The sediment-trap measurements did not start until November 1992 and there were two years in which the sediment trap either malfunctioned (2001) or was lost at sea (2009) (Fig. 1). After formatting the time series into July–June years. there was a total of five incomplete or missing years (1992, 2000, 2001, 2008 and 2009), yielding 16 POC flux years to analyse for the 1993–2013 period. Full results from the 2014-2020 period were not available at the time of this analysis.

To evaluate the phenological timing of the POC flux, an annual peak flux episode (which typically occurs during the austral summer months) was defined to be a period of flux where the daily POC flux was greater than the mean daily (July–June) flux for at least 14 consecutive days⁵³. With this criterion, it was possible to objectively and automatically identify annual peak pulse periods in the POC flux, as well as the initiation and termination dates, and the duration of the annual seasonal pulse. The power spectral density of the full July–June time series was analysed to detect any periodicity in POC flux and to help identify ecological parameters driving the annual cycle, and Bartlett's Kolmogorov–Smirnov statistic⁵¹ was used to test significance.

Environmental and biological comparison

To understand the mechanistic drivers of the POC flux, individual environmental and biological factors affecting the region were compared with temporal patterns in POC flux. Variables analysed include the monthly multivariate ENSO index (MELv2), indices from the National Oceanic and Atmospheric Administration Physical Sciences Laboratory website (https://psl.noaa.gov/enso/mei/), and the monthly SAM index from the British Antarctic Survey (http://www.nerc-bas.ac.uk/icd/gjma/sam.html). Along with full annual and monthly comparisons, August ENSO and SAM indices were also analysed against POC flux, as the peak winter climate greatly affects winter sea ice, a critical component of the MIZ and biological pump⁵⁶.

Daily sea-ice-cover data from 1992 to 2013 were extracted from the NASA Scanning Multichannel Microwave Radiometer and the Defense Meteorological Satellite Programs Special Sensor Microwave/Imager satellite record for the gridded area corresponding to the sediment-trap location (https://doi.org/10.5281/zenodo.7723853), following protocols described in refs. 10,57. Sea-ice cover is at its maximum over the sediment trap during August. The median percentage of August sea-ice cover over this region of interest was calculated for each year and compared with sediment-trap POC flux phenology.

All other oceanographic and biological data analysed in this study are part of the ongoing PAL-LTER time series (https://pallter.marine. rutgers.edu/data/). Each year, data are collected along the WAP during the austral summer (roughly between 1 January and 10 February) when sea-ice cover is near its annual minimum, day lengths are long (with nearly 24 h of sunlight) and biological activity is at its annual maximum. Relevant summer parameters measured during the annual research cruise were compared with the corresponding annual (July–June) POC flux data.

Depth-integrated phytoplankton chlorophyll *a* measurements (https://doi.org/10.6073/pasta/585ba08c3ab00f7d36f3756bb8e7f79b) from the top 100 m of the water column were spatially averaged across the PAL-LTER sample grid points each year and used as a proxy for phytoplankton biomass during peak POC flux periods. Seawater was

collected from vertical profiles along the 500 and 600 PAL-LTER grid lines in Niskin bottles at different depths and was filtered onto GF/F filters and flash frozen for fluorometric phytoplankton chlrophyll a analysis (mg chl a m⁻³) (ref. 22).

E. superba and Salpa thompsoni (salp) abundances (https://doi. org/10.6073/pasta/03e6d72a78bc2512ef5bb327e686f8fa and https:// doi.org/10.6073/pasta/60b41cfa5eaa7298f84b9ac291037403, respectively) and E. superba body size (https://doi.org/10.6073/pasta/2afc 968fad7d40c989de532f52e6720b) were measured on animals collected using a 2-m² frame Metro net (700-µm mesh) towed obliquely to a depth of 120 m at each station https://doi.org/10.6073/pasta/2af c968fad7d40c989de532f52e6720b along the 500 and 600 PAL-LTER grid lines⁴⁰. A General Oceanics flow meter positioned in the centre of the net mouth was used to calculate the volume of seawater filtered⁴⁰. A random subsample of up to 100 E. superba individuals was measured for standard body length (distance between tip of rostrum and blunt end of uropod) for each net tow. For tows containing fewer than 100 individual krill, all E. superba were measured for body size. The body lengths (mm) were assigned to 1-mm-length bins and the median size in each 1-mm-length bin was used in conjunction with the total annual number of krill in each length bin to calculate the weighted summer mean krill body size each year.

E. superba body size was also measured on krill recovered in Adélie penguin (*Pygoscelis adeliae*) diet samples during the summer breeding season in January–February from colonies surrounding Palmer Station (https://doi.org/10.6073/pasta/d0b492b09b678d55db046e27ebe9d1c1). Adélie penguin diet samples were obtained from adult penguins by using the water off-loading method³⁸. Krill from diet samples were measured from the base of the eye to the tip of the telson and placed in 5-mm-length bins. As krill grow >5 mm per year³⁷, these binning methods resolve changes in the krill population size-class structure that occur between years ^{37,39,58}. Seabird diets have been shown to be good proxy indicators of the spatial and temporal variance and structure (length–frequency distribution) of their prey populations⁵⁹. Although Adélie penguin diets represent a high-quality snapshot of the size structure of the krill population each summer, they may not accurately reflect the overall krill abundance.

To examine the annual trends and patterns in the data, we calculated annual standardized anomalies (Zscores) of the POC flux, sea ice, and each biological factor, other than krill body size, to reduce the confounding effects of outlier values and extreme variability, where the mean is subtracted from each value and then divided by the standard deviation of the whole dataset. For annual summer zooplankton abundance anomalies, abundance values were \log_{10} -transformed before calculating annual mean abundance and then Z scores were calculated⁴⁰. Each standardized variable was then compared with the POC flux over the time series through both ordinary least-squares regression and generalized linear models to determine the potential drivers of POC flux.

Data availability

The data analysed in this study can be found at: https://doi.org/10.6073/pasta/cb0ee837fd2615ae133dcfdc0b806571, https://doi.org/10.6073/pasta/d0b492b09b678d55db046e27ebe9d1c1, https://doi.org/10.6073/pasta/2afc968fad7d40c989de532f52e6720b, https://doi.org/10.6073/pasta/03e6d72a78bc2512ef5bb327e686f8fa, https://doi.org/10.6073/pasta/60b41cfa5eaa7298f84b9ac291037403, https://doi.org/10.5281/zenodo.7723853 and https://doi.org/10.6073/pasta/585ba08c3ab00f7d36f3756bb8e7f79b. Bathymetry data can be found at https://doi.org/10.7289/V5C8276M.

- Waters, K. J. & Smith, R. C. Palmer LTER: a sampling grid for the Palmer LTER program. Antarctic J. US 27, 236–239 (1992).
- Ducklow, H. W. et al. Particle export from the upper ocean over the continental shelf of the west Antarctic Peninsula: a long-term record, 1992–2007. Deep Sea Res. Part II 55, 2118–2131 (2008).
- Knap, A., Michaels, A. F., Close, A., Ducklow, H. W. & Dickson, A. Protocols for the Joint Global Ocean Flux Study (JGOFS) Core Measurements (UNESCO, 1994).
- Karl, D. M., Dore, J. E., Hebel, D. V. & Winn, C. in Marine Particles: Analysis and Characterization (eds. Hurd. D. C. & Spencer, D. W.) 71–77 (American Geophysical Union, 1991).
- Kim, H. & Ducklow, H. W. A decadal (2002–2014) analysis for dynamics of heterotrophic bacteria in an Antarctic coastal ecosystem: variability and physical and biogeochemical forcings. Front. Mar. Sci. 3, 214 (2016).
- Martinson, D. G. & Iannuzzi, R. A. in Antarctic Sea Ice: Physical Processes, Interactions and Variability Vol. 74 (ed. Jeffries, M. O.) 243–271 (American Geophysical Union, 1998).
- Siegel, V. & Loeb, V. Length and age at maturity of Antarctic krill. Antarctic. Science 6, 479–482 (1994).
- Reid, K. & Brierley, A. S. The use of predator-derived krill length-frequency distributions to calculate krill target strength. CCAMLR Sci. 8, 155–163 (2001).

Acknowledgements This research was supported by NSF grants OPP 9011927, 9632763, 0217282 2026045, 0823101, and 1440435 for the Palmer Long-Term Ecological Research (PAL-LTER) project. R.T. thanks the NSF Graduate Research Fellowship Program, and the Department of Earth and Environmental Sciences at Columbia University for support. W.R.F. acknowledges support from the Detroit Zoological Society and NSF Office of Polar Programs (ANT-1745018). We are grateful to the officers and crews of the MV Polar Duke and ARSV Laurence M. Gould, and the science and logistics support on the PAL-LTER research cruises This work would not be possible without the PAL-LTER field teams who aided in data collection. We thank D. Karl (University of Hawaii), who started the sediment-trap time series in 1992; T. Houlihan (1992-1997) and C. Carrillo (1998-2002) who supervised University of Hawaii sediment-trap deployments; and N. Shelton (2014-2019) for management efforts, deployment and recovery of Lamont-Doherty Earth Observatory sediment traps. U. Magaard (1992–2002) and H. Quinby (2003-2006) supervised sample analyses at University of Hawaii and VIMS. respectively. We thank J. Cope, M. Gleiber and J. Conroy (Virginia Institute of Marine Science) who compiled and supplied krill data for this analysis: R. Ross and L. Quetin for PAL-LTER krill collection and data before 2009; and PAL-LTER colleagues for discussions.

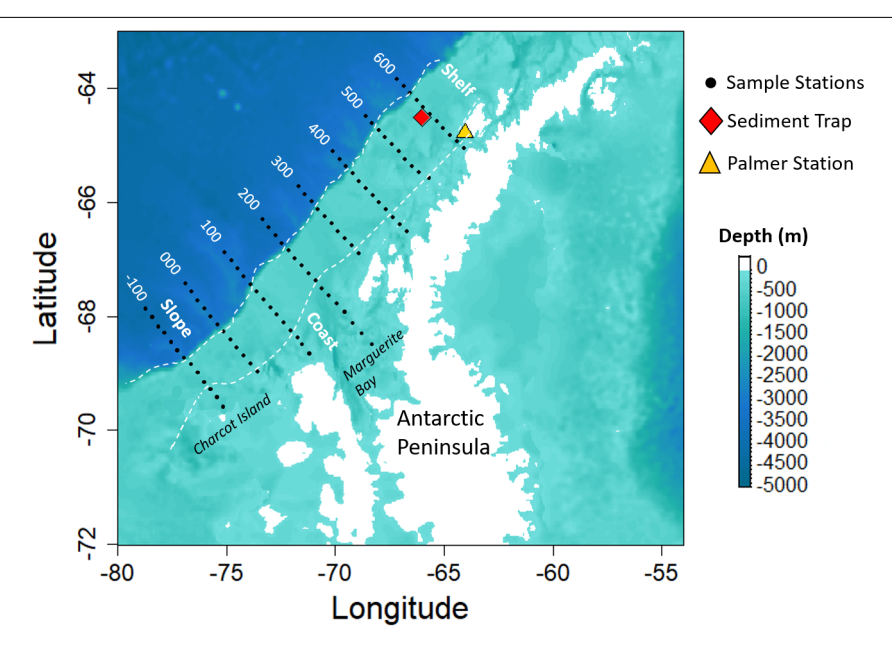
Author contributions R.T.: conceptualization, acquisition of data, formal analysis, visualization, writing—original draft. H.W.D.: conceptualization, acquisition of data, writing—review and editing, funding acquisition. D.K.S.: acquisition of data, writing—review and editing. W.R.F.: acquisition of data, writing—review and editing. R.T., H.W.D., D.K.S. and W.R.F. approved the submitted version for publication.

 $\textbf{Competing interests} \ \mathsf{The \ authors \ declare \ no \ competing \ interests}.$

Additional information

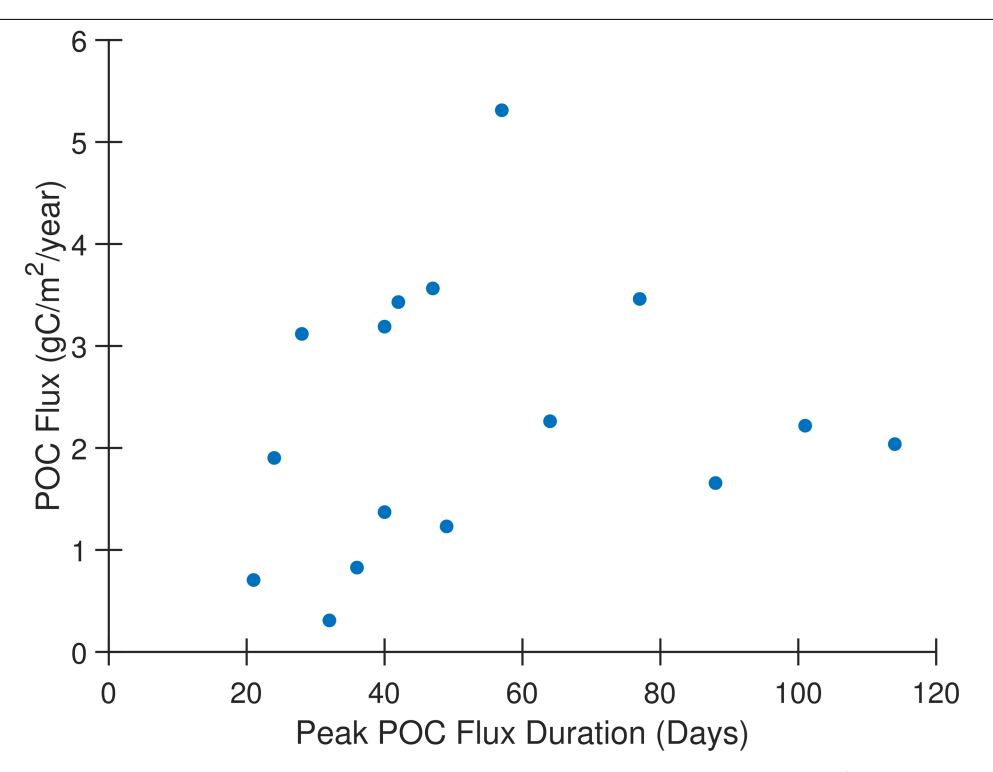
Correspondence and requests for materials should be addressed to Rebecca Trinh. **Peer review information** *Nature* thanks Morten Iversen, Jenan J. Kharbush and Geraint Tarling for their contribution to the peer review of this work.

Reprints and permissions information is available at http://www.nature.com/reprints.

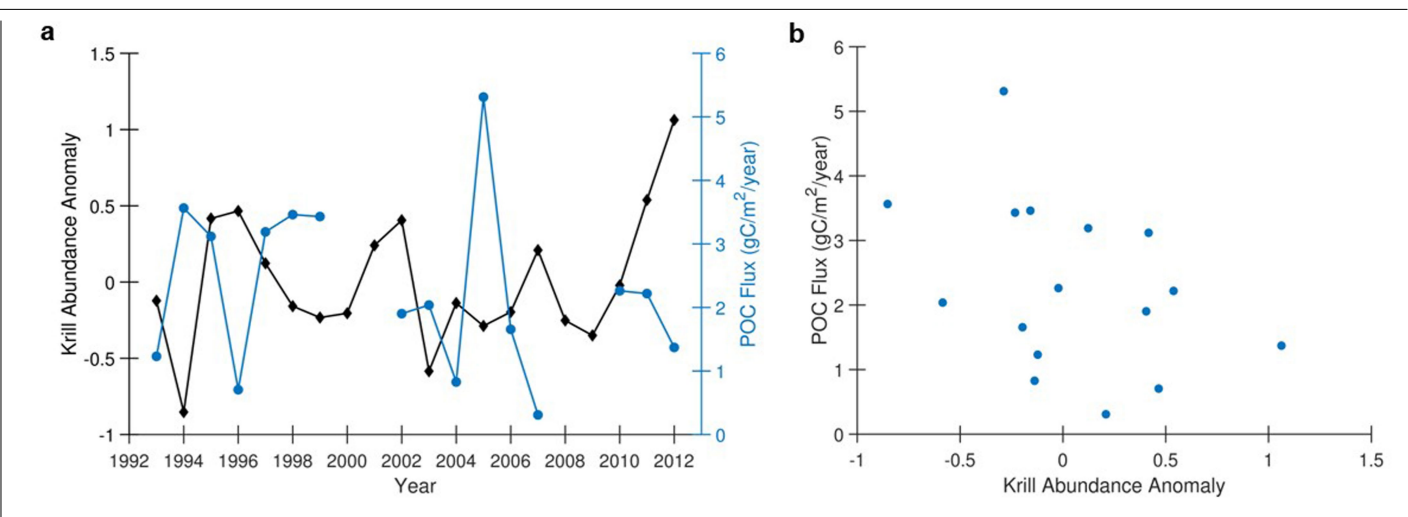


 $\label{lem:extended_DataFig1} \textbf{Bathymetric} \ \textbf{map of the Antarctic Peninsula.} \ \textbf{Location} \ of PAL-LTER sampling stations (black circles) within grid lines labeled -100-600, Palmer Station on Anvers Island (yellow triangle), and long-term sediment trap \ \textbf{matherization} \ \textbf{matherization}$

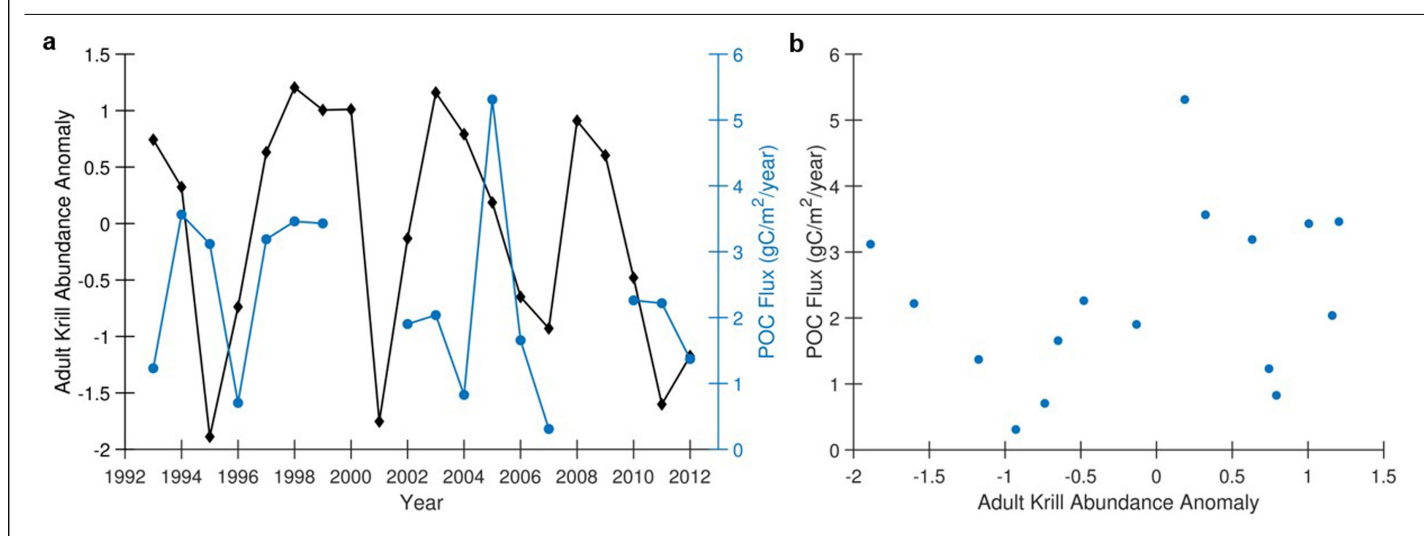
(red diamond), Marguerite Bay, and Charcot Island are shown. White dashed lines separate geographical coast, shelf, and slope regions of the West Antarctic Peninsula.



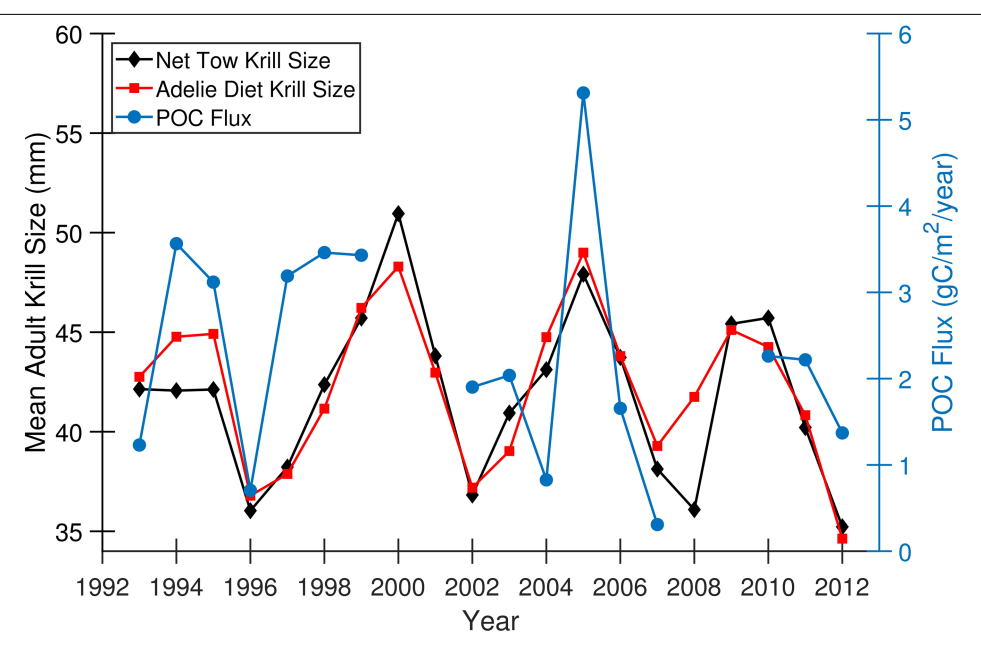
Extended Data Fig. 2 | **Annual POC flux is not a function of peak POC flux duration.** The regression is non-significant ($R^2 = 0.026$, p = 0.54).



Extended Data Fig. 3 | **Annual POC flux does not correlate with total krill abundance. a**) Annual POC flux (blue circles) and total krill abundance anomaly (black diamonds) time series from 1993–2012. **b**) Annual POC flux as a function of total krill abundance anomaly ($R^2 = -0.15$, p = 0.13).

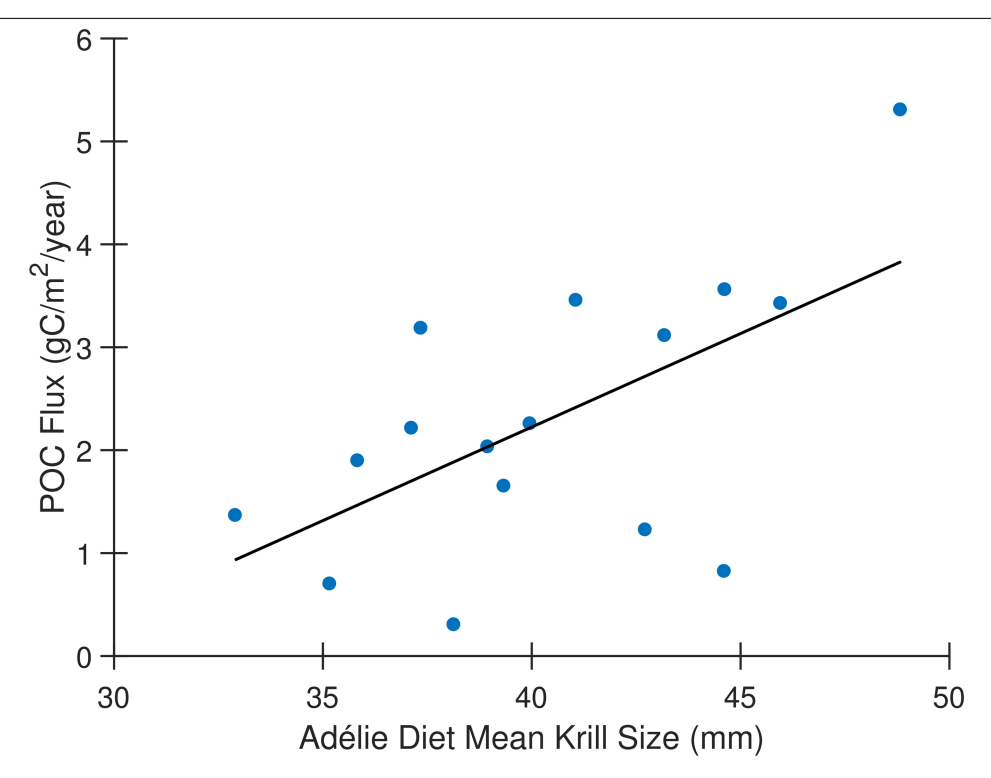


Extended Data Fig. 4 | **Annual POC flux is not driven by adult krill abundance. a**) Annual POC flux (blue circles) and adult krill abundance anomaly (black diamonds) time series from 1993–2012. **b**) Annual POC flux as a function of adult krill abundance anomaly ($R^2 = 0.063, p = 0.35$).

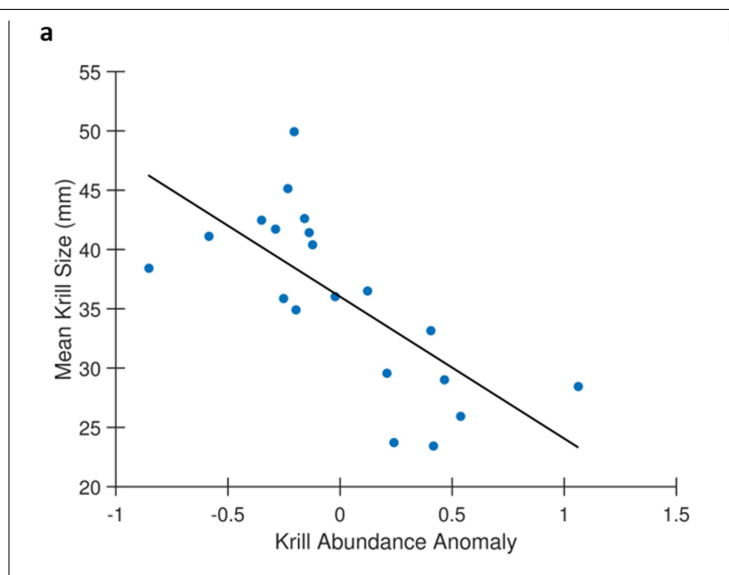


 $\label{lem:extended} \textbf{Extended Data Fig. 5} \ | \ \textbf{Annual POC flux oscillates in sync with adult krill} \\ \textbf{body size obtained through net tows and penguin diets.} \ \textbf{Annual POC flux} \\ (\text{blue circles}), annual mean adult krill body size from net tows (black diamonds),} \\$

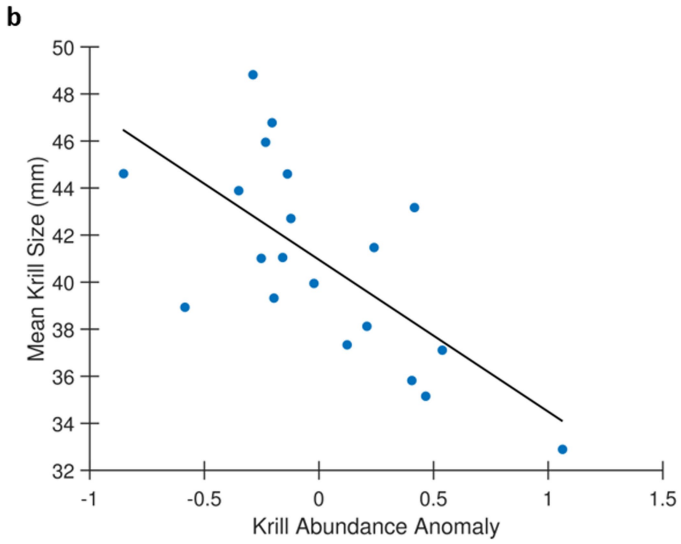
and annual mean adult krill body size from Adélie penguin diets (red squares) time-series from 1993–2012.



Extended Data Fig. 6 | **Penguin derived krill body size and annual POC flux.** Annual POC flux as a function of annual mean adult krill body size from Adélie penguin diet time-series ($R^2 = 0.36$, p = 0.01).



Extended Data Fig. 7 | **Krill body size is negatively correlated with krill abundance.a**) Annual mean krill body size (from net tows) as a function of annual krill abundance ($R^2 = -0.50, p < 0.001$). **b**) Annual mean total krill body



size from Adélie penguin diets as a function of annual total krill abundance anomaly (R^2 = -0.43, p = 0.001).

Extended Data Table 1 | Influence of ecological parameters on POC flux

Parameter	n	R ²	r	p-value
Annual El Niño-Southern Oscillation	16	0.0056	0.0748	0.78
Monthly El Niño-Southern Oscillation	192	0.000002	0.0014	0.98
August El Niño-Southern Oscillation	16	0.005800	0.0762	0.78
Annual Southern Annular Mode	16	0.018	0.1342	0.62
Monthly Southern Annular Mode	192	0.017	0.1304	0.071
August Southern Annular Mode	16	0.077	0.2775	0.30
August Sea Ice Cover Anomaly	16	0.038	0.1900	0.47
Annual Sea Ice Duration Anomaly	16	0.12	0.3464	0.19
Depth-Integrated Chlorophyll-a Anomaly	16	0.11	0.3350	0.20
Salp Abundance Anomaly	16	0.11	0.3366	0.20

 $Linear regression statistics of environmental and biological parameters against annual POC flux over the {\it 21-year time series which showed no significant correlation}.$